The Minimum Period of Oscillation of Simple Tunnel Diode Oscillators

by

D. K. Lynn
R. S. Pepper
D. O. Pederson

Series No. 60, Issue No. 388
AF 49(638)-1043
August 2, 1961

ELECTRONICS RESEARCH LABORATORY
UNIVERSITY OF CALIFORNIA
BERKELEY CALIFORNIA

Electronics Research Laboratory
University of California
Berkeley, California

THE MINIMUM PERIOD OF OSCILLATION OF SIMPLE TUNNEL DIODE OSCILLATORS

by

D. K. Lynn
R. S. Pepper
D. O. Pederson

Institute of Engineering Research
Series No. 60, Issue No. 388

Air Force Office of Scientific Research
of the Air Research and Development Command;
Department of the Navy, Office of Naval Research;
and Department of the Army
Contract No. AF 49(638)-1043

August 2, 1961

ERRATA

Page 9: omitted

ABSTRACT

This report considers the general problem of determining the minimum period of oscillation, regardless of waveshape, for a class of electronic oscillators, one member of which is a tunnel-diode oscillator having a resistive-inductive load. Analysis shows that the minimum period of oscillation is never obtained for a harmonic mode of oscillation. The results are confirmed by experiment.

For the problem at hand, a large-signal (nonlinear) analysis must be made which requires various techniques for solution of the nonlinear problem. A commonly accepted large-signal model for the tunnel diode is used and both piecewise linear and cubic polynomial approximations are used for the tunnel-diode static negative resistance characteristic. Both methods of approximation show that the minimum period of oscillation occurs for the case of zero external inductance and a load resistance equal to zero or approximately equal to zero.

Two methods of solution of the tunnel-diode oscillator equation are used. Computer solutions, involving a piecewise linear approximation to the tunnel-diode negative resistance characteristic are used for cases of highly nonsinusoidal oscillations. If a cubic polynomial approximation to the tunnel-diode negative resistance characteristic is used, analytic solutions are found by means of a perturbation technique (Lindstedt method). From the piecewise linear solutions it is seen that there are many factors that influence the shape of the curve of period of oscillation with the load parameter.

The tunnel diode oscillator may operate as a soft oscillator, hard oscillator, or be truly bistable. The conditions for determining the type of operaton are given.

TABLE OF CONTENTS

LIST OF FIGURES

I. INTRODUCTION

The commonly accepted circuit model of the tunnel diode is shown in Fig. 1. If it is assumed that the tunnel diode operates only in the negative conductance region, the $i = f(v)$ characteristic can be approximated by $i = G_a v$, where G_a is a linear negative conductance. The above assumption requires that the tunnel diode oscillator be a harmonic oscillator*. The minimum period of harmonic oscillation can never be less than

$$T_{min} = \frac{1}{f_c} = 2\pi \frac{C/|G_a|}{\sqrt{\frac{1}{|G_a|R_s} - 1}}$$

The reciprocal of T_{min}, f_c, is sometimes called the cutoff frequency. The usefulness of the above is limited for two reasons. First, there exist some tunnel diodes for which it is not possible to obtain a harmonic or near harmonic oscillation. Second, the above expression is derived from a linear analysis. Consequently, the nonlinear effects of a complete cycle of operation are not included.

The expression above for T_{min} is found from an inspection of the real part of the input impedance of the tunnel diode for sinusoidal frequencies.

$$Z_d(j\omega) = \text{Re } Z_d(j\omega) + ;\text{Imag } Z_d(j\omega)$$

$$= \left(R_s - \frac{|G_a|}{G_a^2 + \omega^2 C^2}\right) + j\left(\frac{-\omega C}{G_a^2 + \omega^2 C^2} + \omega L\right)$$

---

* A pure harmonic oscillation is by definition a single frequency sinusoid. The minimum period rather than the maximum frequency of oscillation is used in this paper to avoid ambiguity for nonharmonic (nonsinusoidal) waveforms. For the latter the frequency of oscillation may be defined as the reciprocal of the period of oscillation, i. e., the frequency of the fundamental Fourier component of the waveform.

If $R_s < \frac{1}{|G_a|}$, a frequency, ω_c, exists where the real part vanishes. If L_s is the proper value, or if inductance can be added as shown in Fig. 2a, such that Imag $Z_d(j\omega_c) = 0$, the circuit consisting of the tunnel diode and a short circuit or the inductive load will oscillate harmonically with a frequency ω_c. For some tunnel diodes, L_s may be too large to accomplish this resonance at ω_c. It is commonly accepted that for such a situation a capacitive load should be introduced to provide the resonance at ω_c as shown in Fig. 2b.[1] However, the total linearized circuit consisting of the tunnel diode and the capacitive load then has an additional natural frequency (a total of three). The added natural frequency may lie in the right half plane. This provides a regenerative mode which may be dominant and lead to a relaxation oscillation when one considers the actual nonlinear circuit operation.* For many available tunnel diodes, this situation arises.

It is evident that the minimum period considerations above are limited since the nonlinear behavior of the circuit is not included. In this paper, attention is centered on the general minimum period problem for the simple tunnel-diode oscillator having a series inductive-resistive load as shown in Fig. 2a. For this circuit, the nonlinear equation which describes the circuit is of second order and available techniques can be used in the analysis.** The problem is to establish the minimum period of oscillation regardless of the wave shape of the oscillation by varying the load's parameters. It is shown that the minimum period does not occur for the harmonic mode of oscillation.

*For a discussion of the bounds in the R. H. P. of natural frequencies for linear active circuits and devices see, E. S. Kuh, "Regenerative Modes of Active Networks", Trans. IRE, Vol CT-7, No. 1, March 1960, and C. A. Desoer and E. S. Kuh, "Bounds on Natural Frequencies of Linear Active Networks", Proc. PIB., Active Networks and Feedback Systems, Vol. 10, pp. 415-436, 1960.

** For the circuit of Fig. 2b, where a capacitive or conductive-capacitive load is used, the nonlinear differential equation describing the circuit is of third order. In general, solutions for equations of third order or higher, must be found for specific element values using numerical techniques.

In Fig. 2a, the labeled elements are as follows:

i = f(v) represents the nonlinear, static i-v characteristic of the tunnel diode as shown in Fig. 1.

C is the diode junction capacitance and is assumed to be a constant.

L_s is the diode lead inductance.

R_s is the diode series resistance.

R_L is the externally added resistance.

L_L is the externally added inductance.

It is convenient to use a suitable transformation of variables to obtain an i'-v' characteristic having a new origin which is in the negative conductance region as shown in Fig. 3b. The circuit model of the oscillator using the new variables is shown in Fig. 3a. Note that $L = L_L + L_s$ and $R = R_L + R_s$. In the work to follow the primes are neglected for simplicity.

II. METHODS OF SOLUTION

The nonlinear differential equation of the circuit in Fig. 3 is

$$\ddot{v} + \left(\frac{R}{L} + \frac{f'(v)}{C}\right)\dot{v} + \frac{v + Rf(v)}{LC} = 0 \qquad (1)$$

where

$$\dot{} = \frac{d}{dt}, \quad f'(v) = \frac{df(v)}{dv}$$

Note that this equation differs from the Van der Pol oscillator equation. The Van der Pol oscillator equation is of the form

$$\ddot{U} + \mu\left(G + f'(U)\right)\dot{U} + U = 0 \qquad (2a)$$

$$\ddot{U} - \epsilon(1 - U^2)\dot{U} + U = 0 \qquad (2b)$$

In the second equation above, the usual cubic approximation is used for the nonlinear i-v characteristic. The minimum period of oscillation for a Van der Pol oscillator described by (2b) is obtained for the harmonic mode. This can be shown by developing an expression for the period as a function of ϵ for ϵ small and ϵ large and joining these

curves.[2, 3, 4] Although this result is true only for the cubic approximation of $i = f(v)$, leading to (2b), it seems reasonable from the work of Haag[5] and Stoker[6] to assume that the harmonic mode also produces the minimum period of oscillation for a piecewise linear approximation for $i = f(v)$.

In contrast to the Van der Pol equation, note in (1) that both the v and $\dot{v}$ terms contain coefficients that are functions of the dependent variable. Hence, the conclusion concerning the minimum period of oscillation just drawn for the Van der Pol oscillator cannot be applied.[7]

A number of methods are available for the solution of (1). For particular values or graphs of the circuit elements, graphical phase-plane analysis can be used to establish a limit cycle. From the limit cycle, information as to the output period and output waveshape may be obtained. However, inherently low accuracy of the phase plane method is undesirable in treating the minimum period problem. Furthermore, it is difficult from graphical analysis of specific examples to draw general conclusions as to the conditions for obtaining the minimum period of oscillation.

In this paper two other methods of solution are used. The first method is to use a three segment piecewise linear approximation to the $i = f(v)$ characteristic and to solve the resulting mixed boundary condition problem using a digital computer. The second method is to use a polynomial approximation for $i = f(v)$, e. g., $f(v) \approx -\alpha v + \gamma v^3$ and obtain an expansion for the reciprocal of the period as a function of the parameters of the $i = f(v)$ approximation and the fixed circuit elements. Such expansions can be found by means of the Lindstedt method[8] and are valid for the case of nearly harmonic oscillations.

A piecewise linear approximation to the $i = f(v)$ characteristic is shown in Fig. 3c. Because of the linear segments or portions of operation, a complete period of oscillation can be separated into active and decay modes. When the voltage, v, in Fig. 3c has a value $-v_o \leq v \leq v_o$, the circuit is said to be in the active mode. In the active mode the $i = f(v)$ characteristic is considered as a linear negative conductance of value G_a. When the voltage has a value $|v| > v_o$, the

circuit is said to be in the decay mode. In the decay mode the i = f(v) characteristic is considered as a linear positive conductance of value G_d together with a Thevinen equivalent voltage source. For simplicity the two positive conductance regions of the i = f(v) characteristic are assumed to have the same slope. Note that for a complete cycle of operation, two excursions are made in the active mode and one excursion in each of the decay modes.

The characteristic equations of the circuit in Fig. 3a during the active mode and decay modes are:

Active mode:

$$\ddot{v}_1 + \left(\frac{R}{L} + \frac{G_a}{C}\right)\dot{v}_1 + \frac{1}{LC}(1 + RG_a)v_1 = 0 \qquad (3a)$$

Decay mode:

$$\ddot{v}_2 + \left(\frac{R}{L} + \frac{G_d}{C}\right)\dot{v}_2 + \frac{1}{LC}(1 + RG_d)v_2 = 0 \qquad (3b)$$

Equations (3a) and (3b) are linear equations; therefore, we may introduce magnitude and frequency (time) normalizations such that the normalized values of L and C are unity, i. e., $L_n = C_n = 1$. These normalizations simplify the solutions. The characteristic equations become

Active Mode:

$$v_1'' + (R_n + G_{an})v_1' + (1 + R_nG_{an})v_1 = 0 \qquad (4a)$$

Decay Mode:

$$v_2'' + (R_n + G_{dn})v_2' + (1 + R_nG_{dn})v_2 = 0 \qquad (4b)$$

where $0' = \frac{d}{dt}$; R_n, G_{an}, G_{dn} are the normalized values of R, G_a, and G_d respectively.

Since both (4a) and (4b) are linear equations, the concept of natural frequencies of a specific mode can be used. It is seen later that the loci of these natural frequencies are a great aid in establishing the possible performance of the oscillator. The natural frequencies of the active and decay modes are

Active Mode:

$$p_{0,1} = \frac{-(R_n + G_{an})}{2} \pm \frac{\sqrt{(R_n - G_{an})^2 - 4}}{2} \qquad (5a)$$

Decay Mode:

$$p_{2,3} = \frac{-(R_n + G_{dn})}{2} \pm \frac{\sqrt{(R_n - G_{dn})^2 - 4}}{2} \qquad (5b)$$

The possible loci of the natural frequencies in the complex frequency plane of both modes are plotted in Fig. 4 for typical values of G_{an} and G_{dn} as the parameter R_n is varied.

It can be seen in Fig. 4b that the natural frequencies for the active mode may cross the $j\omega$ axis. At the point where these loci cross the $j\omega$ axis a pure harmonic mode is obtained. Notice also that for certain values of G_{an} ($|G_{an}| > 1$) the loci of the natural frequencies as shown in Fig. 4a do not cross the $j\omega$ axis for nonzero values of ω. For this case it is clear that a harmonic oscillation is impossible to obtain regardless of the value of the parameter R_n.

III. COMPUTER SOLUTIONS

Through the use of digital computers the period of oscillation can be determined as the parameters R_n, G_{dn}, and G_{an} are varied. For convenience we normalize the $i = f(v)$ curve so that the active mode exists for $-1 \leq v \leq 1$, i.e., in Fig. 3c $v_o = 1$. The general solution for the active mode, (4a) is

$$v_1(\tau_a) = C_0 e^{p_o \tau_a} + C_1 e^{p_1 \tau_a}, \quad p_0 > p_1 \qquad (6)$$

$$|v_1| \leq 1$$

The general solution for the decay mode, (4b), is

$$v_2(\tau_d) = -v_3(\tau_d) = C_2 e^{p_2 \tau_d} + C_3 e^{p_3 \tau_d} + C_4$$

$$v_2 < -1, \quad v_3 > 1 \qquad (7)$$

It is to be emphasized that separate time origins are used for each mode. The mode sequence for a complete period is chosen as follows:

Active 1 $v_1(0) = +1$ to $v_1(\tau_1) = -1$

Decay 1 $v_2(0) = -1$ to $v_2(\tau_2) = -1$, $\tau_2 \neq 0$

Active 2 $v_1(0) = -1$ to $v_1(\tau_1) = +1$

Decay 2 $v_3(0) = +1$ to $v_3(\tau_2) = +1$, $\tau_2 \neq 0$

Because of the symmetry of the complete solution, only the first two modes need be considered. The constants C_0, C_1, C_2 and C_3 are unknown constants to be determined from the boundary or matching conditions of the problem. These conditions are that voltage and its derivative are matched at the boundary of active and decay modes, and that the solutions be periodic. The constant C_4 in (7) is a known constant which can be found from examining the equivalent circuit.

$$C_4 = \frac{G_{an} - G_{dn}}{G_{dn} + 1/R_n} \tag{8}$$

Data has been obtained on a computer which gives the time in the active mode, τ_1, the time in the decay mode, τ_2, and the total period, $T = 2(\tau_1+\tau_2)$, for various values of G_{an}, G_{dn}, and R_n. The normalized values chosen for G_{an} are -.5, -1.5, and -5. This choice was made to obtain the three distinct loci of the natural frequencies in the active mode as shown in Fig. 5. A ratio of $N = -G_{dn}/G_{an}$ between 1 and 6 satisfies the f(v) characteristics of commercially available tunnel diodes; therefore, the values of N used for this study were chosen to be N = 1, 3, and 6.

A summary of the results for $G_{an} = -5$ is presented in Table 1 and in the curves of Fig. 6. The loci of the natural frequencies of the active and decay modes are also shown in Fig. 6. It is to be noted that for this case, the natural frequencies of the active mode do not have a $j\omega$ axis

crossover except at the origin. It is seen that the minimum period of oscillation occurs for $R_n = 0$. A physical explanation for this is as follows. In the decay mode, for the chosen values of N, the natural frequencies are always real; therefore, $v_2(\tau_d)$ decays monotonically toward C_4. If sustained oscillations are to exist, C_4 must be greater (more positive) than -1. This is evident from an examination of $v_2(\tau_d)$ shown in Figs. 7a and 7b. From (8) it can be seen that as R increases towards $-1/G_{an}$, C_4 decreases toward -1. Consequently, the time in the decay mode increases rapidly as R_n approaches $-1/G_{an}$. In addition, the time in the active mode also increases. This is a result of the rapid decrease of $v_1'(0) = -v_2'(\tau_2)$ caused by the asymptotic approach of $v_2(\tau_d)$ to -1, cf, the slope of curve a, Fig. 7. For R_n greater than $-1/G_{an}$, C_4 is less than - 1, and the circuit will never get out of the decay mode and back into the active mode, cf, curve b, Fig. 7. Hence, sustained oscillations are not obtained.

A summary of the results for $G_{an} = -1.5$ is presented in Table 2 and in the curves of Fig. 8. The loci of the natural frequencies of the active and decay modes are also shown in Fig. 8. It can be seen that the minimum period of oscillation does not occur exactly for $R_n = 0$. However, the value of T_{min} is not much different from T for $R_n = 0$. The factors influencing the shape of T vs R_n curve in this case are more complex than in the previous case. For a value of R_n greater than 0.5, the natural frequencies in the active mode are real, and the shape of the T vs R_n curve for this range is explained by the same reasons as given above for $G_{an} = -5$. This is even true for N = 1 ($G_{dn} = 1.5$) where the natural frequencies in the decay mode are complex. For the latter, however, the natural frequencies lie near the 135 and 225 degree radials, and the decay mode solutions do not have large oscillatory terms. The initial decrease of T for R_n increasing from zero is explained by the decrease of τ_2, the decay time. This effect could be anticipated from the loci of the natural frequencies in the decay mode. For example, note that for N = 3 and 6, the natural frequency in the decay mode which is nearest the origin for $R_n = 0$ steadily moves away from the origin as R_n increases. This indicates a tendency for τ_2

to decrease. In contrast, the time in the active mode, τ_1, continually increases as is expected from the nature of the loci of the natural frequencies in the active mode, i.e., both the real and imaginary parts of $p_{0,1}$ decrease as R_n increases from zero. Eventually the increase in τ_1 is dominant over the decrease of τ_2, and a minimum in the T vs R_n curve results.

Computer results for $G_{an} = -.5$ are not listed. For this situation, the active mode natural frequencies may cross the jω axis at non zero values of ω. The main result of the computer solutions for $G_{an} = -.5$ was to show that the minimum period should occur for small values of R_n and not at the jω axis crossover. For N = 3, the approximate minimum period is 6.4. The accuracy of the results was somewhat in doubt, however, since the method of computer solution that was used created a convergence problem when the solutions became almost harmonic. There may also be a problem due to the fact that since the oscillations are nearly harmonic and of small amplitude, the piecewise linear approximation to i = f(v) may be in considerable error due to the sharp break points at $v = \pm 1$. Consequently, an analytic solution for the period in the neighborhood of harmonic solutions is used.

The question can now be answered as to the effects of adding inductance in the load. In the above work, normalized values of parameters were used. In particular,

$$G_{an} = G_a \text{ - normalized} = G_a \text{ - actual } \sqrt{\frac{L \text{ actual}}{C \text{ actual}}}$$

$$T = T \text{ - normalized} = T \text{ actual} / \sqrt{L \text{ actual } C \text{ actual}}$$

As inductance is added, G_{an} becomes larger. From Table 3 it is seen that the normalized minimum period becomes larger as G_{an} increases. The actual minimum period will, of course, be even larger after denormalizations. Consequently, the conclusion can be drawn that the minimum period is obtained when no load inductance is added and the load is a pure resistance of a certain value.

TABLE 3

$G_{an} = 0.5$,	$N = 6$	$T_m = 6.60$
0.5,	$N = 1$	$T_m = 6.35$
$G_{an} = 1.5$,	$N = 1$	$T_m = 6.92$
	$N = 3$	$T_m = 8.16$
	$N = 6$	$T_m = 8.96$
$G_{an} = 5$,	$N = 3$	$T_m = 17.52$
	$N = 1$	$T_m = 12.94$
	$N = 6$	$T_m = 19.76$

IV. ANALYTIC SOLUTIONS

To obtain an analytical solution to (1) the $i = f(v)$ characteristic is approximated by $i = -\alpha v + \gamma v^3$ and use is made of the Lindstedt method, a perturbation technique. The result is a solution for the period as a function of the parameters of the problem. The details of the Lindstedt method are given in the Appendix A. The final results are:

$$\frac{2\pi}{T} = \omega_1 = \frac{\beta_o}{\sqrt{LC}} \left[1 + \frac{R\sqrt{\frac{C}{L}}}{2\beta_o^2} \epsilon - \frac{1}{16\beta_o^2} \left(1 + \frac{3R^2 \frac{C}{L}}{\beta_o^2}\right) \epsilon^2 \right]$$

where $\alpha < \sqrt{\frac{C}{L}}$, $\epsilon \geq 0$

$$\beta_o^2 = 1 - \alpha R, \quad \epsilon = \alpha\sqrt{\frac{L}{C}} - R\sqrt{\frac{C}{L}}$$

Note that $\alpha < C/L$ and $\epsilon \geq 0$ includes all possible cases of non zero $j\omega$ axis crossings of the roots of the characteristic equation of the linearized oscillator. The constraint that $\alpha < \sqrt{C/L}$ implies that $0 \leq \epsilon < 1$. Thus for any value of α, L, C, and R, providing $\alpha < \sqrt{C/L}$ and $\epsilon \geq 0$ the expression for the period, T, as given by (9) should be quite accurate. The first two terms of (9) are the most important, and it is shown below

that the contribution due to the ϵ^2 term is usually of the order of a few percent. An examination of the first two terms of (9) reveals that $\left.\frac{d\omega}{dR}\right|_{\epsilon = 0} < 0$.

Thus the minimum period of oscillation is not obtained for $\epsilon = 0$, i.e., the harmonic mode. In particular, it can be shown that considering only the first two terms of (9) the minimum period of oscillation occurs for R = 0.

To establish the effect of higher order terms of (9), evaluations of the ϵ^2 term were made using a digital computer. For representative cases the contribution from the ϵ^2 term was approximately 5 percent or less. Therefore, if the contribution from the ϵ^2 term is included, the minimum period of oscillation occurs for R slightly greater than zero. Since $R = R_s + R_L$, the minimum period of oscillation for $\epsilon \geq 0$ and $a < \sqrt{C/L}$ will occur for $R_L \approx 0$ ($R = R_s$). Furthermore, an examination of each of the terms of (9) clearly shows that the minimum period of oscillation occurs for the minimum value of L, i.e., $L = L_s$. For the analytical solution this result is consistent with those obtained for the piecewise linear solutions.

V. BISTABILITY AND HARD OSCILLATIONS

In section 3 it is stated that for the example of $G_{an} = -5$ oscillations ceased when R_n was increased to a value $-\frac{1}{G_{an}}$. In general, as R_n is increased to a value greater than $-\frac{1}{G_{an}}$, at least one active mode natural frequency moves into the LHP, and C_4 becomes less than -1. When the active mode natural frequencies are real and $R_n = -\frac{1}{G_{an}}$, the circuit makes a transition from a soft oscillator to either a hard oscillator or a bistable circuit. This is explained below.

The dc load line may intersect the i = f(v) characteristic at one or three points. For a single intersection as shown in Fig. 9, it can be shown that both natural frequencies of the active mode are in the right half plane and the circuit is ac unstable.* Therefore, oscillations

* This is shown by putting the condition for one intersection of the dc load line and the i = f(v) characteristic into (6). From this, one can show that unless the natural frequencies of the active mode are real, with one in the LHP and the other in the RHP, there is only one intersection of the dc load line and the i = f(v) characteristic.

will build up spontaneously. This is what is referred to as a soft oscillation. It is possible, however, to achieve oscillations when one of the natural frequencies of the active mode is in the right half plane and the other is in the left half plane. In this situation the dc load line intersects the i = f(v) characteristic in three places as shown in Fig. 10. Two of these intersections are stable. This situation may lead to so-called hard oscillations, that is, if the circuit is initially at rest at one of the two stable points, a sufficiently large excitation of the circuit may result in self sustaining oscillations.

Inspection of the constant C_4 enables one to rule out the possibility of hard oscillations for many cases. If the decay mode has two real natural frequencies, and if the value of C_4 is less than -1 (more negative) no self sustaining oscillations can exist. One then has true bistability. The conditions on G_{an} and R_n for this are:

$$C_4 = -1 = \frac{G_{an} - G_{dn}}{G_{dn} + 1/R_n}$$

$$R_n = -\frac{1}{G_{an}} \qquad (10)$$

$R_n = -1/G_{an}$ is the condition for the natural frequency, p_1, to move to the origin. Consequently, no hard oscillations are possible for real decay mode natural frequencies.

If the decay mode has a pair of complex natural frequencies, the problem is more difficult. In this case, even though C_4 is less than -1, the oscillatory part of the decay solution may carry $v_2(\tau_d)$ to the edge of the active mode and self sustained oscillations may occur cf, Curve (c), Fig. 7. In Appendix B, a method is given to solve for conditions necessary for hard oscillations.

Since a hard oscillator requires an excitation to start it oscillating, it is of interest to know just how much of an input must be supplied. This can be accomplished by constructing a phase portrait in the phase

plane. For hard oscillations, an unstable limit cycle is present.* This limit cycle is a locus of points such that if operation is started outside this locus, self sustained oscillations will occur. If the excitation is such that the initial point is inside this locus, the circuit will settle to one of its stable points. Limit cycles for a hard and soft oscillator are shown in Fig. 11.

VI. EXPERIMENTAL RESULTS

Experimental oscillators have been built using a germanium tunnel diode with a static i-v characteristic as shown in Fig. 12a. From this and other measurements one finds the following characteristics for the tunnel diode

$L_s = 6 \times 10^{-9}$ h

$C = 7$ pf

$R_s = 1 - 1.5\ \Omega$

$\alpha = -G_a = 4.6 \times 10^{-3}$ mho.

In Fig. 12b the actual i-v characteristic of the tunnel diode is repeated and the cubic and piecewise linear approximations used for the Lindstedt and piecewise linear solutions respectively are included. For both methods of approximation a bias point of 150 mv was chosen. A value of $N = \frac{G_{dn}}{-G_{an}} = 4.9$ was used for the piecewise linear approximation. From the figure it is seen that the piecewise linear approximation is quite good in the positive resistance region on the left and in the negative resistance region, but there is considerable error for the positive resistance region on the right. A four segment piecewise linear approximation might be used to obtain a better fit by using the extra segment in the valley region.

The cubic approximation tends to spread the error more evenly on the left and the right, but it is difficult to say whether this leads to a better overall approximation.**

---

* A closed curve, C, in the phase plane is called an unstable limit cycle if it is approached by trajectories, C; both from the inside and the outside for $t = -\infty$.

** A quadratic term was added to the cubic approximation to give a closer approximation to the actual i-v characteristic. The assumed form then became $i = -\alpha v + \beta v^2 + \gamma v^3$. It was found, however, that by using the Lindstedt method, the term βv^2 had no effect on the frequency to first order in ϵ.

The first oscillator was constructed to verify the Lindstedt and piecewise linear analysis techniques for the case of almost harmonic oscillations. For the case chosen, $L = 50L_s$, which resulted in a normalized conductance, G_{an}, of -.954. In Fig. 13 is shown a graph of normalized period, T, versus normalized resistance, R_n, for both the Lindstedt and piecewise linear analysis techniques, as well as the experimentally obtained curves. Two experimental curves are given to illustrate the effect of a change in the bias point. The bias of 130 mv corresponds to operation about the center of the negative resistance region of the static i-v characteristic.

The second oscillator was constructed to verify the piecewise linear analysis technique for the case of nonharmonic oscillations. For this example a normalized value of $G_{an} = -1.75$ was used. This choice of G_{an} required L to be 1.011×10^{-6} Henry. In Fig. 14 is shown a graph of normalized period versus normalized resistance for the piecewise linear analysis technique and for the experimentally obtained curves. Again two bias points are used for the experimental curves as explained above.

From an examination of Figs. 13 and 14 it is seen that the agreement between the experimental and analytic curves is adequate considering the approximations involved in the analyses. In addition, the agreement between the Lindstedt and piecewise linear solutions in Fig. 13 is quite good considering the wide difference in the two methods of solution.

VII. CONCLUSIONS

This paper considers a simple tunnel-diode oscillator having a resistive-inductive load. Using both piecewise linear and cubic approximations to the tunnel-diode static i-v characteristic, we have shown that the minimum period of oscillation of the tunnel-diode oscillator under consideration is never obtained when the oscillator is adjusted for the highest frequency in the harmonic mode. Furthermore, for the piecewise linear approximation, if the natural frequencies in

the active mode are real for all values of R, then for representative values of $N = G_{dn}/G_{an}$ the minimum period of oscillation is obtained for $R_L = 0$ or $R_L \approx 0$. These results are in contrast with a Van der Pol oscillator for which the minimum period of oscillation is achieved for the harmonic mode. Finally, it is seen that adding any external inductance serves to lengthen the period of oscillation.

Two methods of solution of the tunnel-diode oscillator equation have been used. Computer solutions, involving a piecewise linear approximation to the $i = f(v)$ characteristic, have been used for cases of highly nonsinusoidal oscillations. Analytic solutions, using the Lindstedt method, have been used for cases of nearly sinusoidal oscillations. From the piecewise linear solution, it can be seen that there are many factors that influence the shape of the T vs R curve. Some of these factors are related to the loci of the natural frequencies of a particular mode. For the analytical solutions, the $i = f(v)$ characteristic is approximated by a cubic polynomial, $i = -\alpha v + \gamma v^3$. Additional terms could be added to the polynomial to achieve a better fit to the actual $i = f(v)$ characteristic. For such approximations, the Lindstedt method could still be used, but with correspondingly more effort. As mentioned above, the addition of a term βv^2 to the cubic approximation had no effect on the frequency (period) to first order in ϵ.

It has been seen that the agreement between the experimental and analytic curves of T versus R_n is adequate considering the approximations involved in the piecewise linear and Lindstedt methods of solution.

The tunnel diode may operate as a soft oscillator, hard oscillator, or be truly bistable. The conditions for determining the type of operation are given.

As a final point, this study suggests a related problem. An interesting and practical problem is to determine the conditions for maximum output power at a given sinusoidal frequency or alternately to determine the condition for the minimum period of oscillation for a given fundamental power output.

Table I

$G_a = -5$

G_{dn}	N	R_n for T_{min}	T_{min}
5	1	0.0	12.94
15	3	0.0	17.50
30	6	0.0	19.76

Table II

$G_a = -1.5$

G_{dn}	N	R_n for T_{min}	T_{min}	T for R = 0
1.5	1	.05	6.92	6.94
4.5	3	.05	8.16	8.20
9.0	6	.15	8.82	8.96

APPENDIX A: THE LINDSTEDT METHOD

Consider the following nonlinear differential equation

$$\ddot{X} + \Omega^2 X + \epsilon f(x, \dot{x}) = 0 \qquad \text{(A-1)}$$

We assume that it has a periodic solution. Equation (A-1) is to be solved by the Lindstedt method for sufficiently small ϵ. * It is desired to find a periodic solution x(t), with a certain unknown period, T. A new independent variable is first introduced.

$$\tau = \frac{2\pi t}{T} = \omega t \qquad \text{(A-2)}$$

* The convergence of the Lindstedt method is a very difficult question. Although it is customary to assume convergence, Poincaré has shown by an example that the series can diverge.

Equation (A-1) becomes

$$\omega^2 X'' + \Omega^2 X + \epsilon f(x, \omega\dot{x}) = 0 \qquad \text{(A-3)}$$

where $' = d/d\tau$

Next it is assumed that the solution $X(\tau)$ can be written in the form

$$X(\tau) = \sum_{n=0}^{\infty} \epsilon^n \psi_n(\tau) \qquad \text{(A-4)}$$

where the ψ_n are periodic functions with period 2π. The ψ_n are represented by their Fourier series. In addition, assume ω has the form

$$\omega = \sum_{n=0}^{\infty} \beta_n \epsilon^n \qquad \text{(A-5)}$$

where the β_n are constants.

A substitution of these series expansions for ω and $X(\tau)$ is made and a series of recurrent differential equations is obtained which results from equating to zero the coefficients of equal powers of ϵ. It is convenient to choose the time origin such that

$$\left(\frac{dX(\tau)}{d\tau}\right)_{\tau=0} = \left(\frac{d\psi_n(\tau)}{d\tau}\right)_{\tau=0} = 0 \qquad \text{(A-6)}$$

The method of Lindstedt consists of determining the coefficients β_n in the subsequent stages of the recurrence procedure so as to eliminate terms with the fundamental period 2π. These terms, if left in, would lead to so-called secular terms, i.e., terms of the form

$$\tau^n \sin\tau, \quad \tau^n \cos\tau \qquad \text{(A-7)}$$

These terms must be eliminated since one requires the series represent the solution for $0 \leq \tau < \infty$.

The Lindstedt method is now applied to the tunnel-diode oscillator. First approximate the static $i = f(v)$ characteristic by

$$i = f(v) = -\alpha v + \gamma v^3, \quad \alpha > 0, \ \gamma > 0 \qquad \text{(A-8)}$$

After substitution of (A-8) into (1), one obtains:

$$\ddot{v} + \left(\frac{R}{L} + \frac{-a + 3\gamma v^2}{C}\right)\dot{v} + \frac{v + (-a v + \gamma v^3)R}{LC} = 0 \qquad \text{(A-9)}$$

It is necessary to put (A-9) into the form of (A-1). In particular, a parameter must be found for the expansions such that when this parameter equals zero, the solutions are that of a harmonic oscillator. The proper form of (A-1) is obtained using the following in (A-9).

$$\tau' = \frac{1}{\sqrt{LC}}\, t \qquad \text{(A-10)}$$

$$\epsilon = \frac{a L - RC}{\sqrt{LC}} \qquad \text{(A-11)}$$

$$v = h X \qquad \text{(A-12)}$$

$$h^2 = \frac{\epsilon\sqrt{C/L}}{3\gamma} \qquad \text{(A-13)}$$

The result is:

$$X'' + X(1 - a R) = \epsilon\left[(1 - X^2)X' - \frac{RX^3}{3}\right] = \epsilon f(X, X') \qquad \text{(A-14)}$$

where $' = d/d\tau'$

We now use (A-2). The basic equation becomes

$$\omega^2 X'' + X(1 - a R) + \epsilon\left[\frac{R}{3}X^3 + \omega X^2 X' - \omega X'\right] = 0 \qquad \text{(A-15)}$$

where $' = d/d\tau$

Equations (A-4) and (A-5) are introduced and the time origin is chosen using (A-6).
The result of equating to zero the coefficients of equal powers of ϵ gives

$$\epsilon^0: \beta_0^2\psi_0'' + \psi_0(1 - \alpha R) = 0 \qquad \text{(A-16)}$$

$$\epsilon^1: \beta_0^2\psi_1'' + \psi_1(1 - \alpha R) + 2\beta_0\beta_1\psi_0'' + \frac{R}{3}\sqrt{\frac{C}{L}}\,\psi_0^3 + \beta_0\psi_0^2\psi_0' - \beta_0\psi_0' = 0 \qquad \text{(A-17)}$$

$$\epsilon^2: \beta_0^2\psi_2'' + \psi_2(1-\alpha R) + 2\beta_0\beta_1\psi_1'' + (\beta_1^2 + 2\beta_0\beta_2)\psi_0'' + \beta_0\psi_0^2\psi_1' + \beta_1\psi_0^2\psi_0' + 2\beta_0\psi_0\psi_1\psi_0' - \beta_0\psi_1' - \beta_1\psi_0' + R\sqrt{\frac{C}{L}}\,\psi_0^2\psi_1 = 0 \qquad \text{(A-18)}$$

Solving (A-16), one obtains

$$\psi_0 = a_0 \cos\tau \qquad \text{(A-19)}$$

$$\beta_0^2 = 1 - \alpha R \qquad \text{(A-20)}$$

These results are substituted into (A-17) and several trigonometric identities are used to obtain:

$$\beta_0^2(\psi_1' + \psi_1) = \beta_0\left[\frac{a_0^3}{4} - a_0\right]\sin\tau + \left[2a_0\beta_0\beta_1 - \frac{\sqrt{\frac{C}{L}}\,Ra_0^3}{4}\right]\cos\tau - \frac{\sqrt{\frac{C}{L}}\,Ra_0^3}{12}\cos 3\tau + \frac{\beta_0 a_0^3}{4}\sin 3\tau \qquad \text{(A-21)}$$

The secular terms are removed by choosing

$$a_0 = 2 \qquad \text{(A-22)}$$

$$\beta_1 = \frac{R\sqrt{\frac{C}{L}}}{2\beta_0} = \frac{R\sqrt{\frac{C}{L}}}{2\sqrt{1 - \alpha R}} \qquad \text{(A-23)}$$

Equation (A-21) now reduces to

$$\beta_0^2(\psi_1'' + \psi_1) = 2\beta_0 \sin 3\tau - \frac{2}{3} R\sqrt{\frac{C}{L}} \cos 3\tau \qquad \text{(A-24)}$$

The general solution of (A-24) which also satisfies (A-6) is

$$\psi_1 = \frac{3}{4\beta_0} \sin\tau - \frac{1}{4\beta_0} \sin 3\tau \frac{R\sqrt{\frac{C}{L}}}{12\beta_0^2} \cos 3\tau + p \cos\tau \qquad \text{(A-25)}$$

Putting the previous results into (A-18), applying several trigonometric identities, and removing the secular term, one finds

$$\beta_2 = \frac{-3}{16} \frac{R^2 \frac{C}{L}}{\beta_0^3} - \frac{1}{16\beta_0} \qquad \text{(A-26)}$$

$$p = \frac{-R\sqrt{\frac{C}{L}}}{6\beta_0^2} \qquad \text{(A-27)}$$

The expressions just found for β_0, β_1, and β_2, are now used to find ω.

$$\omega = \beta_0 \left[1 + \frac{R\sqrt{\frac{C}{L}}}{2\beta_0^2} \epsilon - \frac{1}{16\beta_0^2} \left(1 + \frac{3R^2 \frac{C}{L}}{\beta_0^2}\right) \epsilon^2 \right] \qquad \text{(A-28)}$$

where $\alpha < \sqrt{\frac{C}{L}}$, $\epsilon \geq 0$

$$\beta_0^2 = 1 - \alpha R, \quad \epsilon = \alpha\sqrt{\frac{L}{C}} - R\sqrt{\frac{C}{L}}$$

The proper time denormalization can be introduced to obtain the expression for the actual period.

$$\frac{2\pi}{T} = \omega_1 = \frac{\omega}{\sqrt{LC}} \qquad \text{(A-29)}$$

APPENDIX B: BISTABILITY AND HARD OSCILLATIONS

Whether the circuit will be bistable or be a hard oscillator can be determined by a study of the piecewise linear solution. The circuit is either bistable or a hard oscillator if and only if one active mode natural frequency, p_0, is located on the positive real axis and the other, p_1, is located on the negative real axis. In (6), therefore, the term $C_1 e^{p_1 \tau_a}$ decays to zero with time. Consequently, given $v_1(0) = 1$, the initial state of the mode must be such that C_0 is negative. For the investigation of the border line situation, assume $C_0 < 0$ and $0 < |C_0| \ll 1$. The time in the active mode, τ_1, is then large and

$$v_1(\tau_a) \approx C_0 e^{p_0 \tau_a} \tag{B-1}$$

Since $v_1(\tau_1) = -1$:

$$\tau_1 = \frac{1}{p_0} \ln\left(\frac{-1}{C_0}\right) \tag{B-2}$$

$$\dot{v}_1(\tau_1) = -p_0$$

these values can be used together with the decay mode solution to establish the condition for self-sustained oscillation. For the decay mode, the discussion in section 5 indicates that it is necessary to have complex decay natural frequencies. Equation (7) can then be written as follows and the matching condition with the first active mode can be included, i.e., $v_2(0) = v_1(\tau_1)$, $\dot{v}_2(0) = \dot{v}_1(\tau_1)$

$$v_2(\tau_d) = -A_2 e^{\sigma_2 \tau_d} \sin(\omega_2 \tau_d + \phi_2) + C_4 \tag{B-3}$$

where

$$\phi_2 = \tan^{-1} \frac{-\omega_2(1 + C_4)}{\sigma_2(1 + C_4) - p_0}$$

If it exists, τ_2 is found from a solution of the transcendental equation (B-3) using $v_2(\tau_2) = -1$, $\tau_2 \neq 0$. The final condition to be satisfied for a self-sustaining oscillation is found from

$$C_0 = \frac{\dot{v}_1(0) - p_1}{p_0 - p_1} < 0, \quad v_1(0) = 1 \qquad \text{(B-4)}$$

Since $-\dot{v}_2(\tau_2) = \dot{v}_1(0)$, the necessary condition is

$$-\dot{v}_2(\tau_2) < p_1 \qquad \text{(B-5)}$$

A procedure to investigate whether (B-5) can be satisfied can be developed for a computer. Thus, the existence of a self-sustained oscillation can be established for a given example.

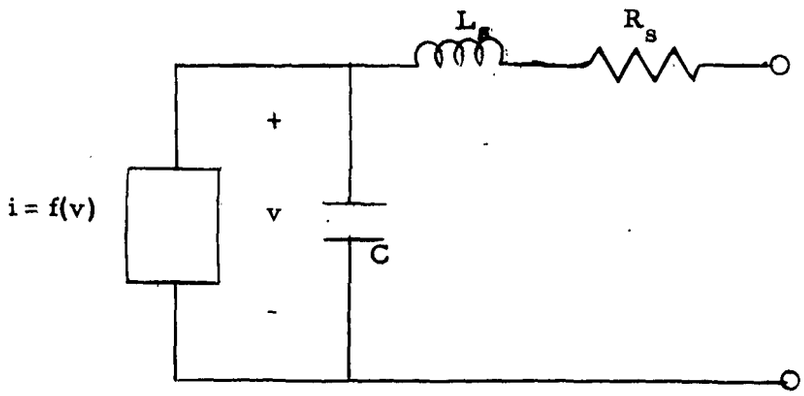

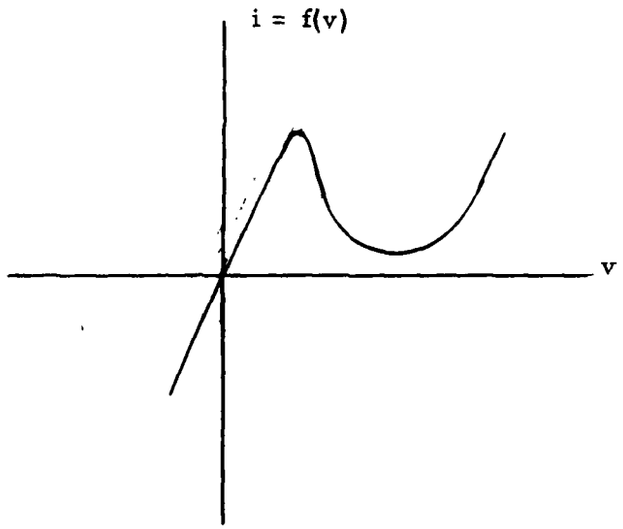

Figure 1 Tunnel Diode Circuit Model

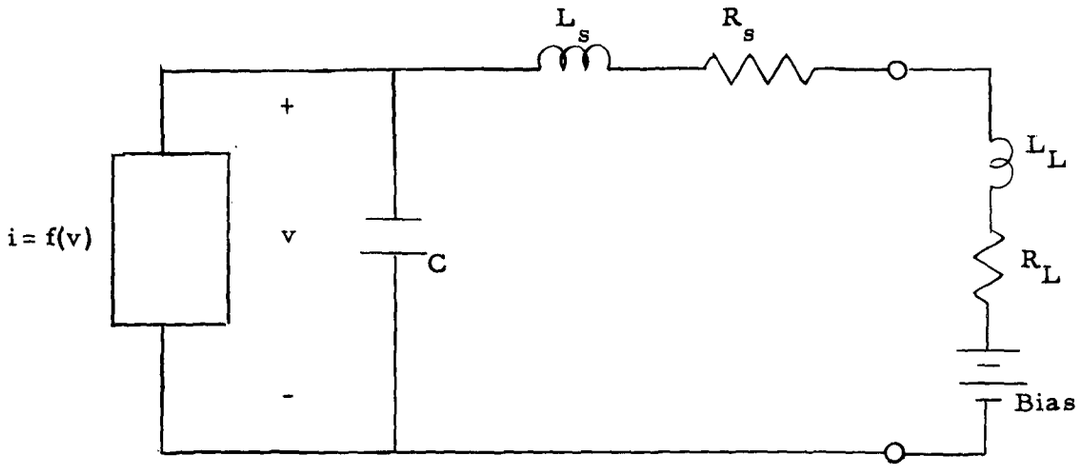

(a)

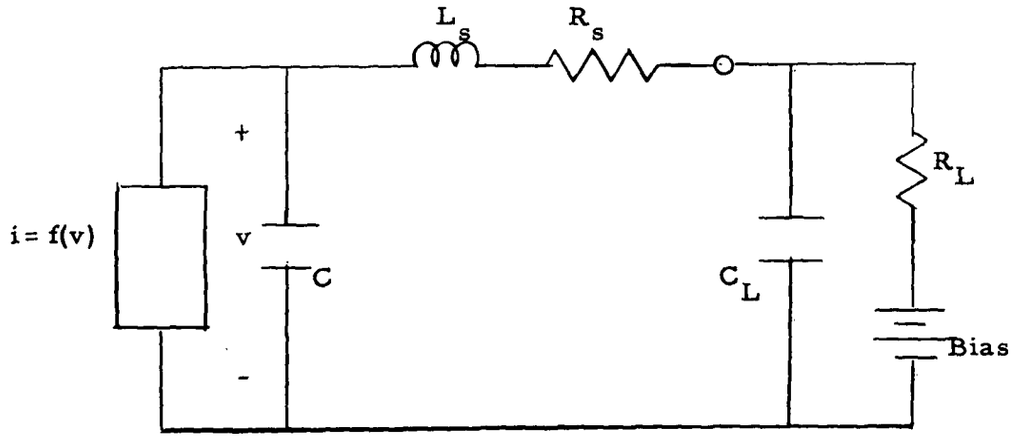

(b)

Figure 2 Tunnel Diode with Load and Bias

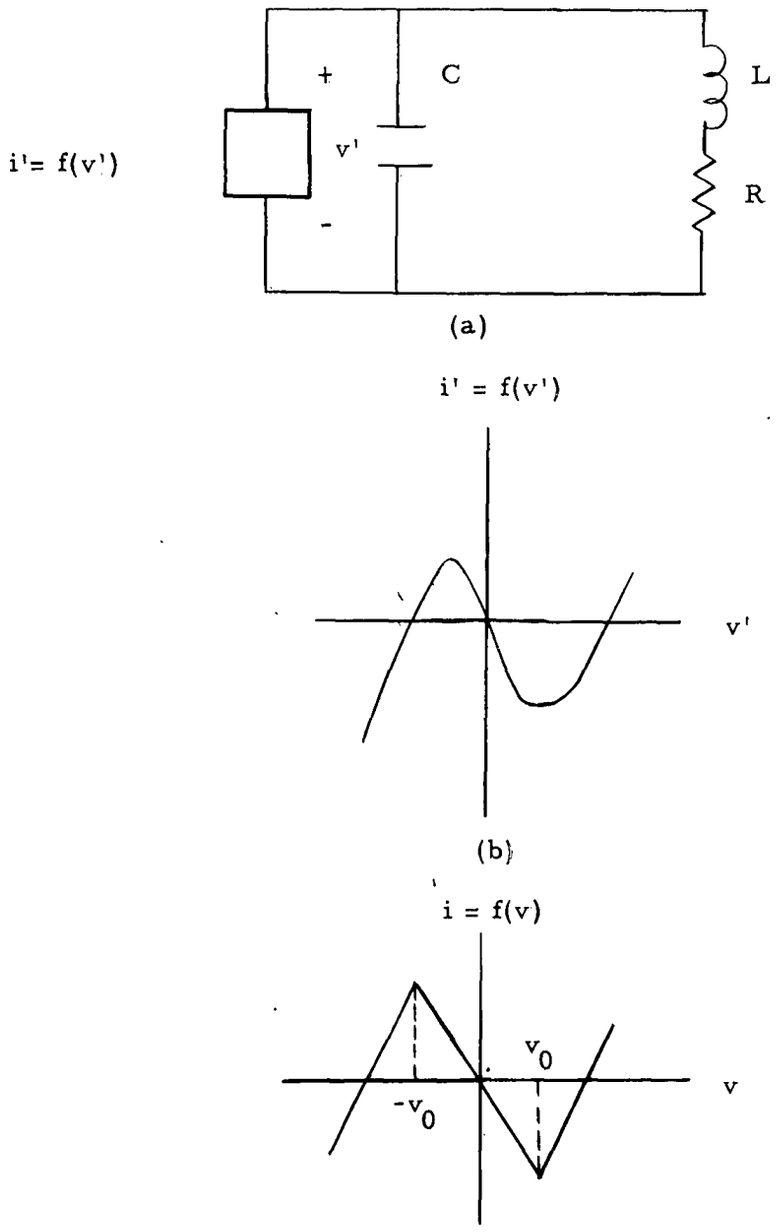

Figure 3 Tunnel Diode Oscillator

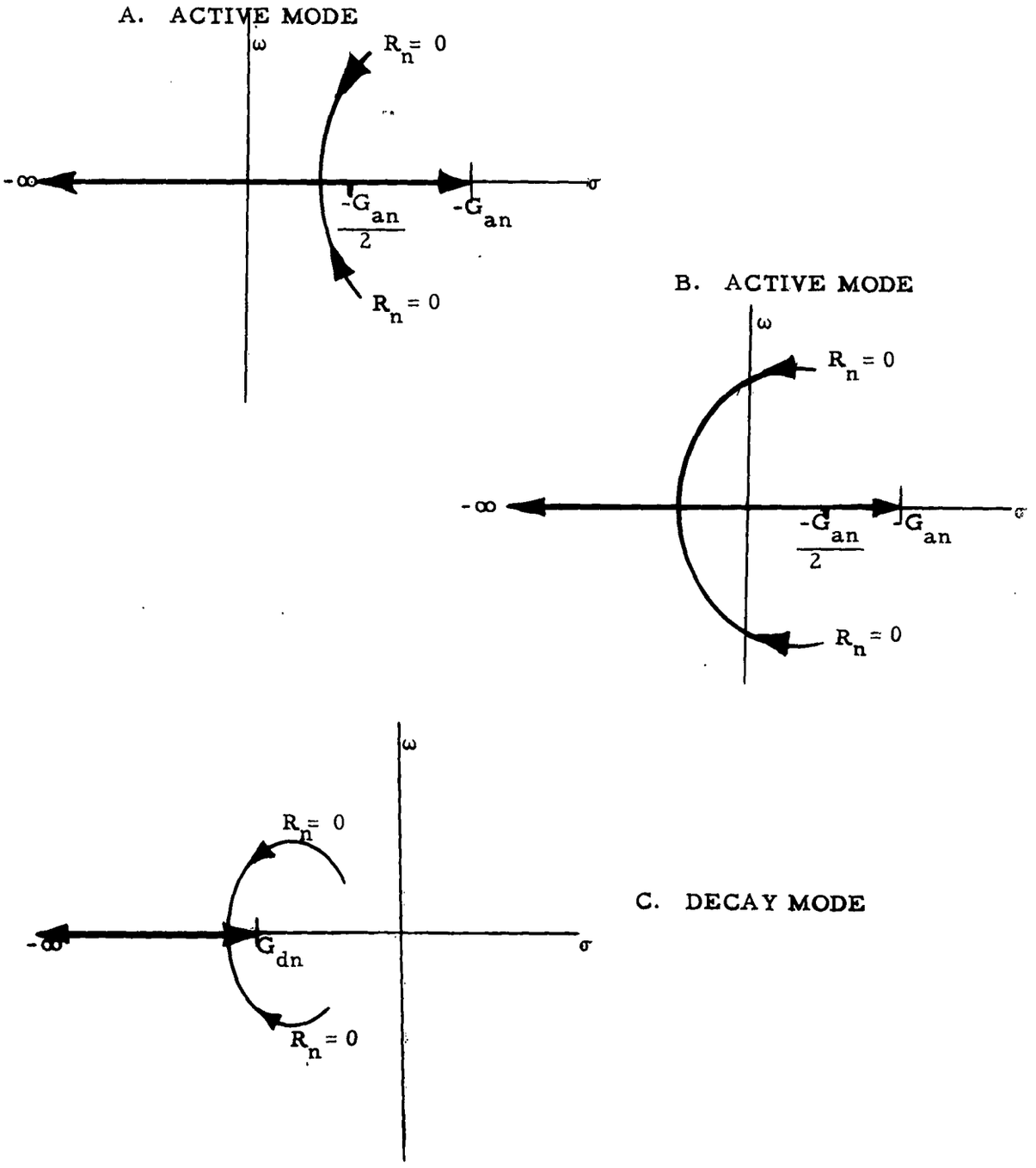

Figure 4 Loci of Natural Frequencies

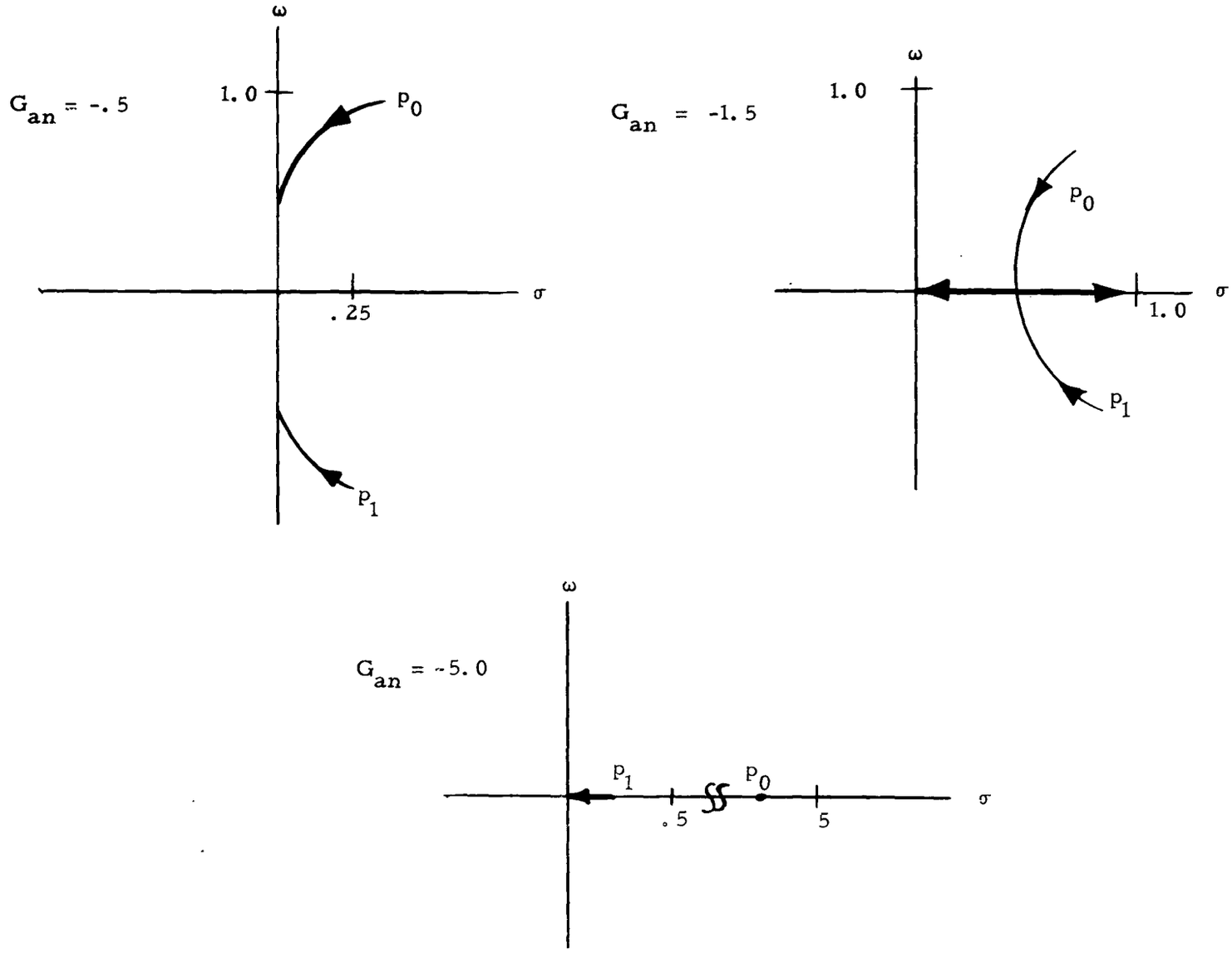

Figure 5 Loci of Natural Frequencies

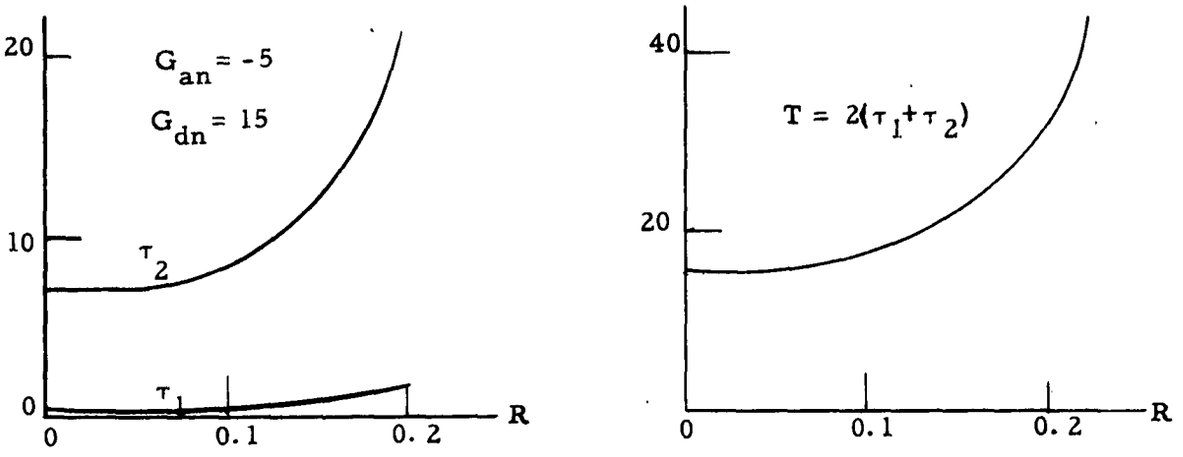

Computer Results for Piecewise Linear f(v)

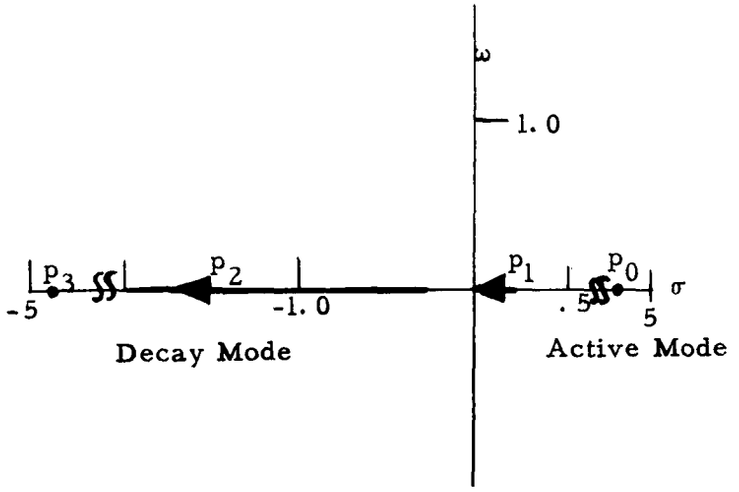

Loci of Natural Frequencies

Figure 6

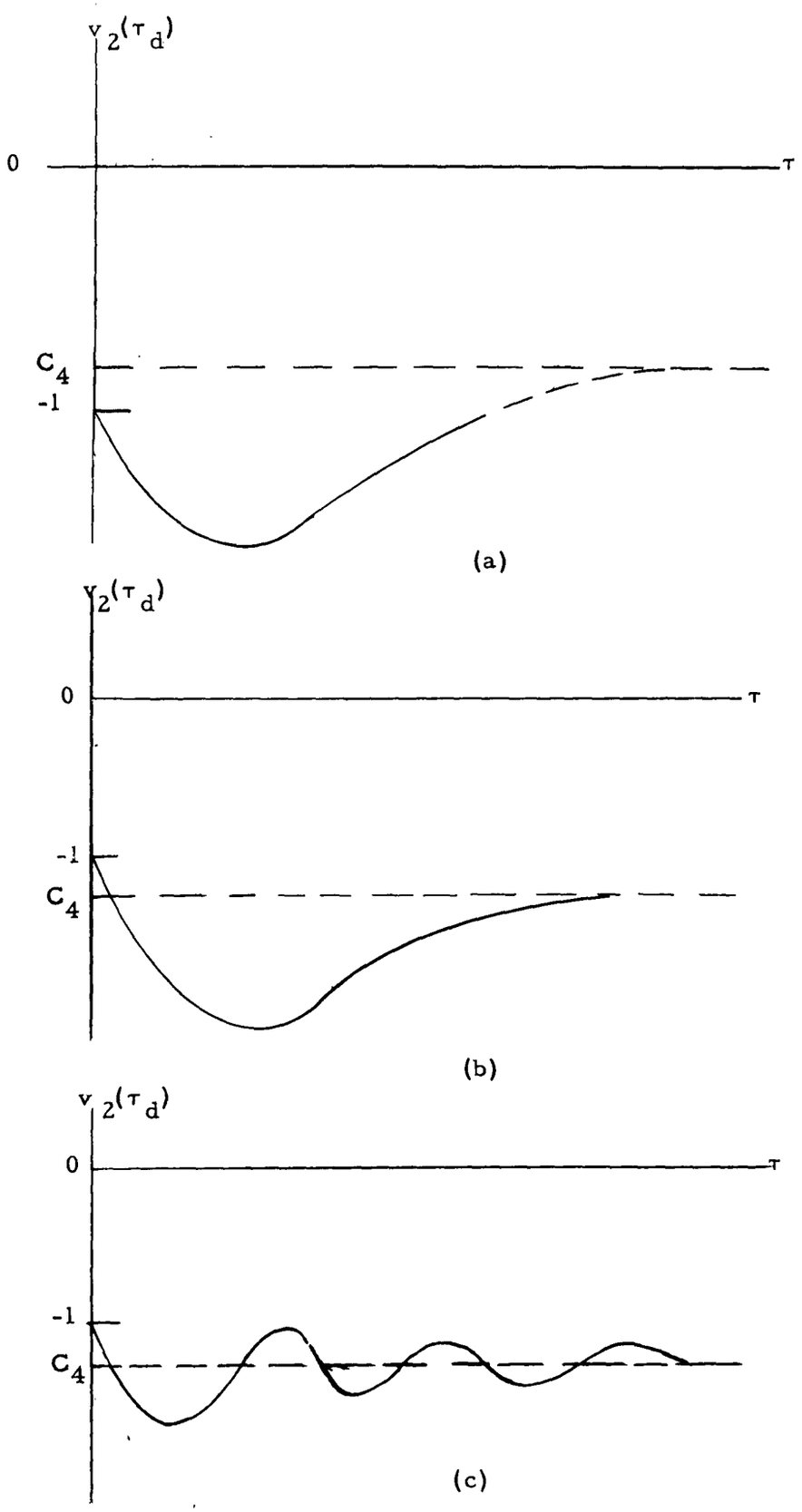

Figure 7 Plot of Possible Voltage Responses in the Decay Mode

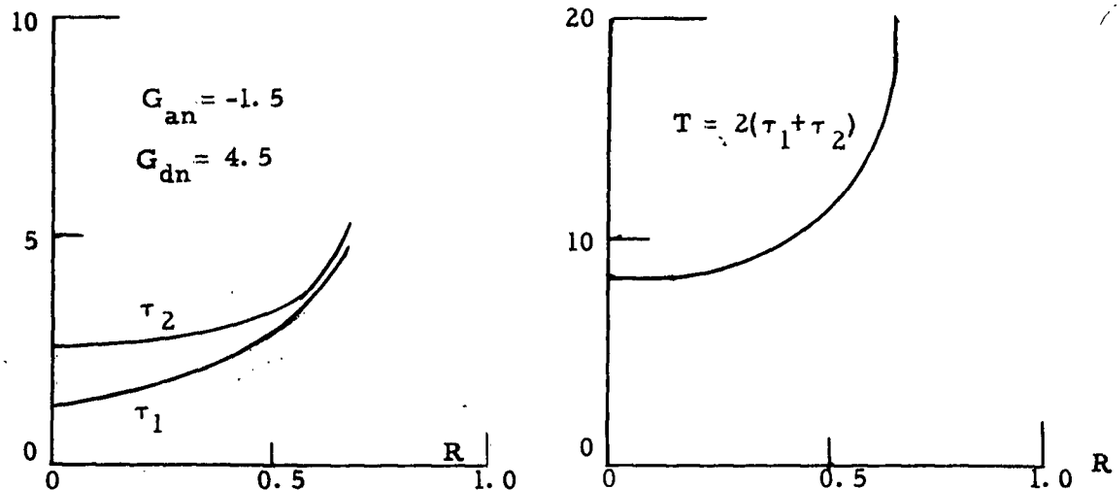

Computer Results for Piecewise Linear f(v)

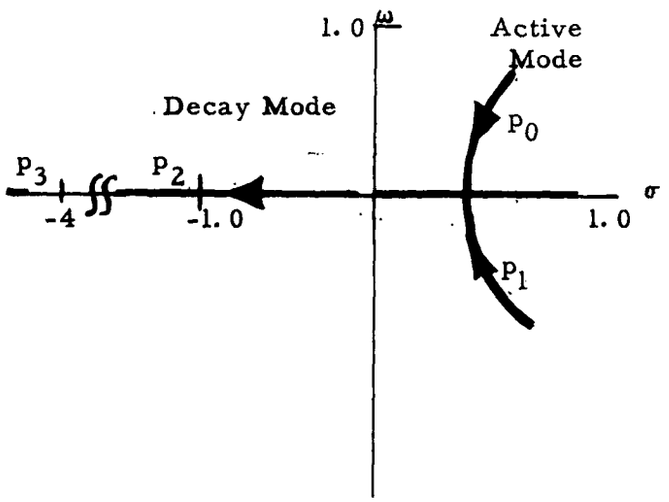

Loci of Natural Frequencies

Figure 8

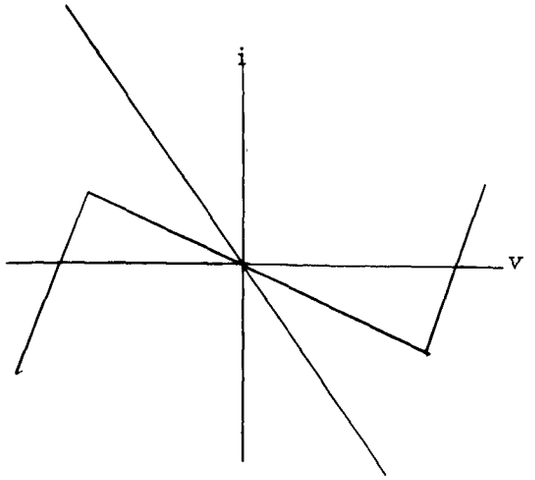

Figure 9 DC Load Lines

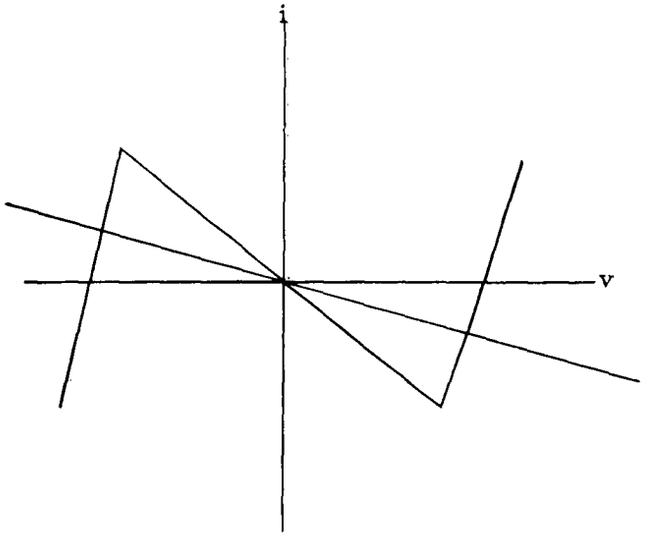

Figure 10 DC Load Lines

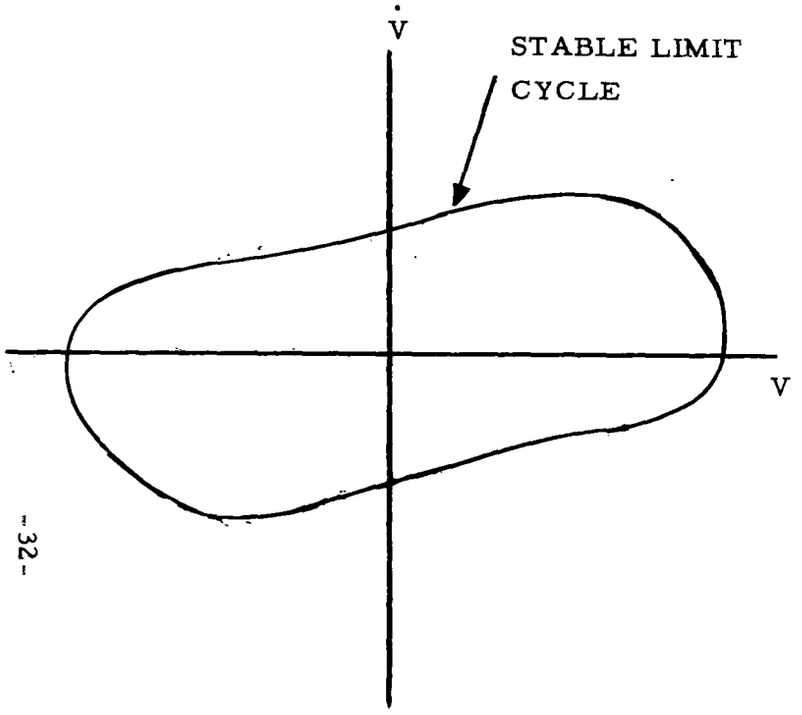

SOFT OSCILLATOR

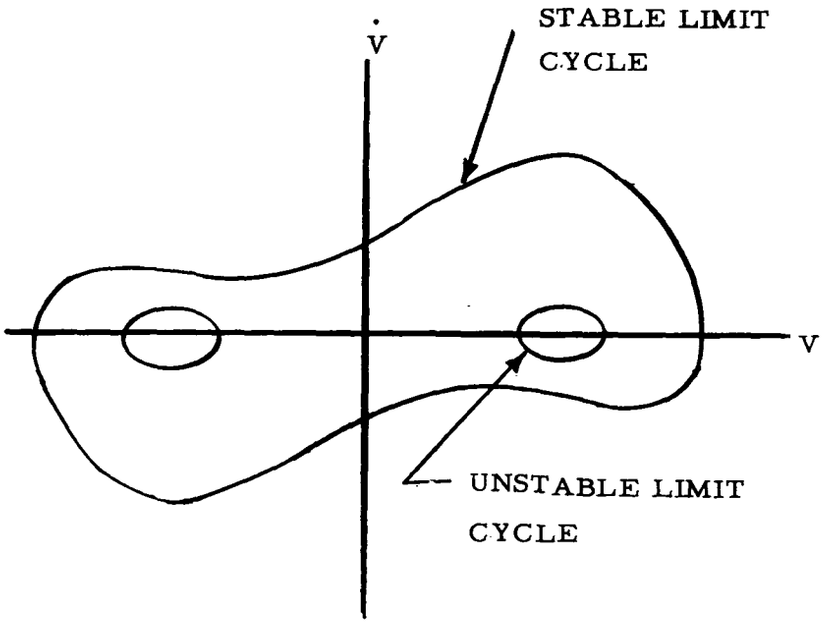

HARD OSCILLATOR

PHASE PLANE PORTRAITS

Figure 11

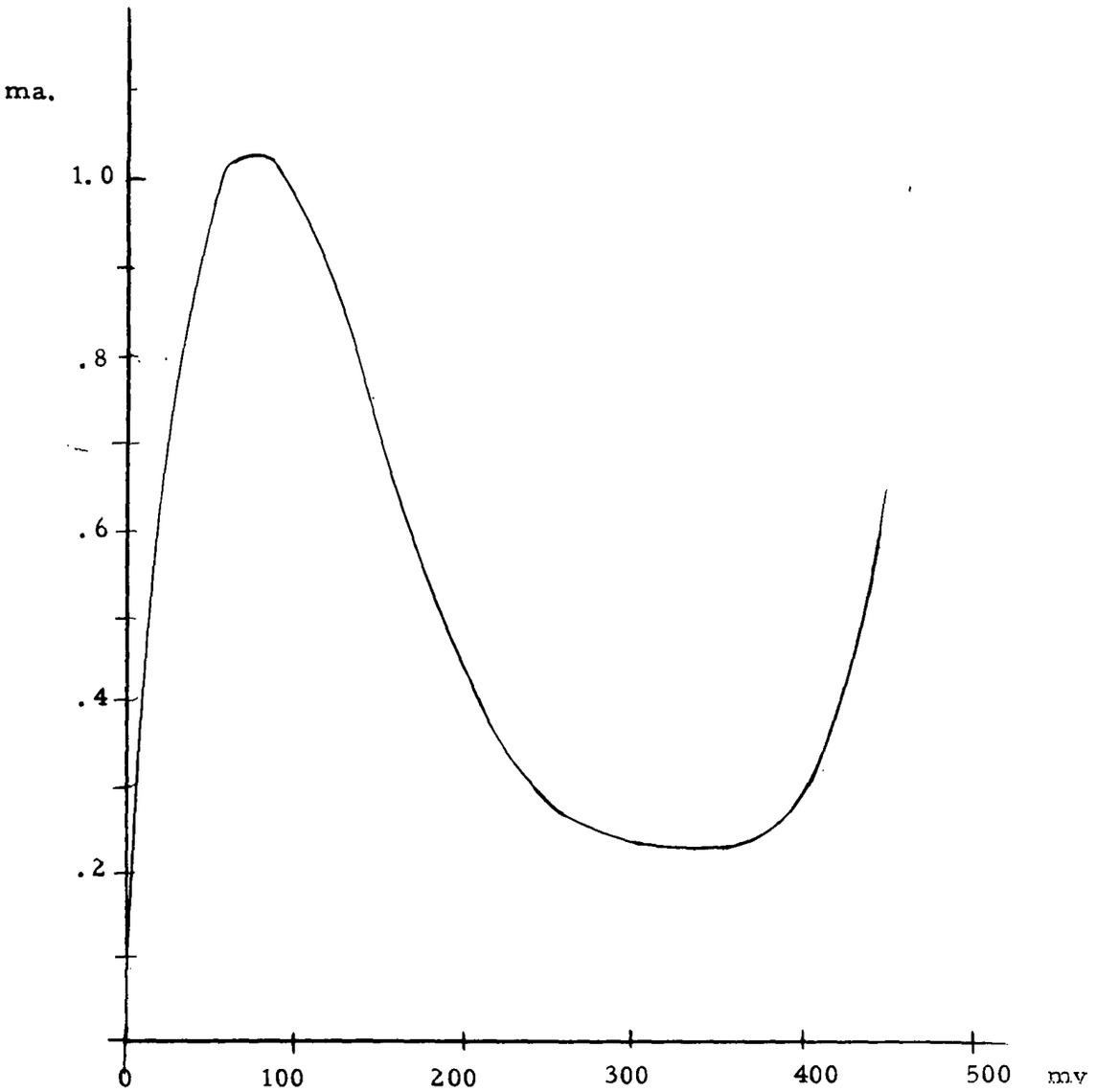

Figure 12a Actual Static i-v Characteristic

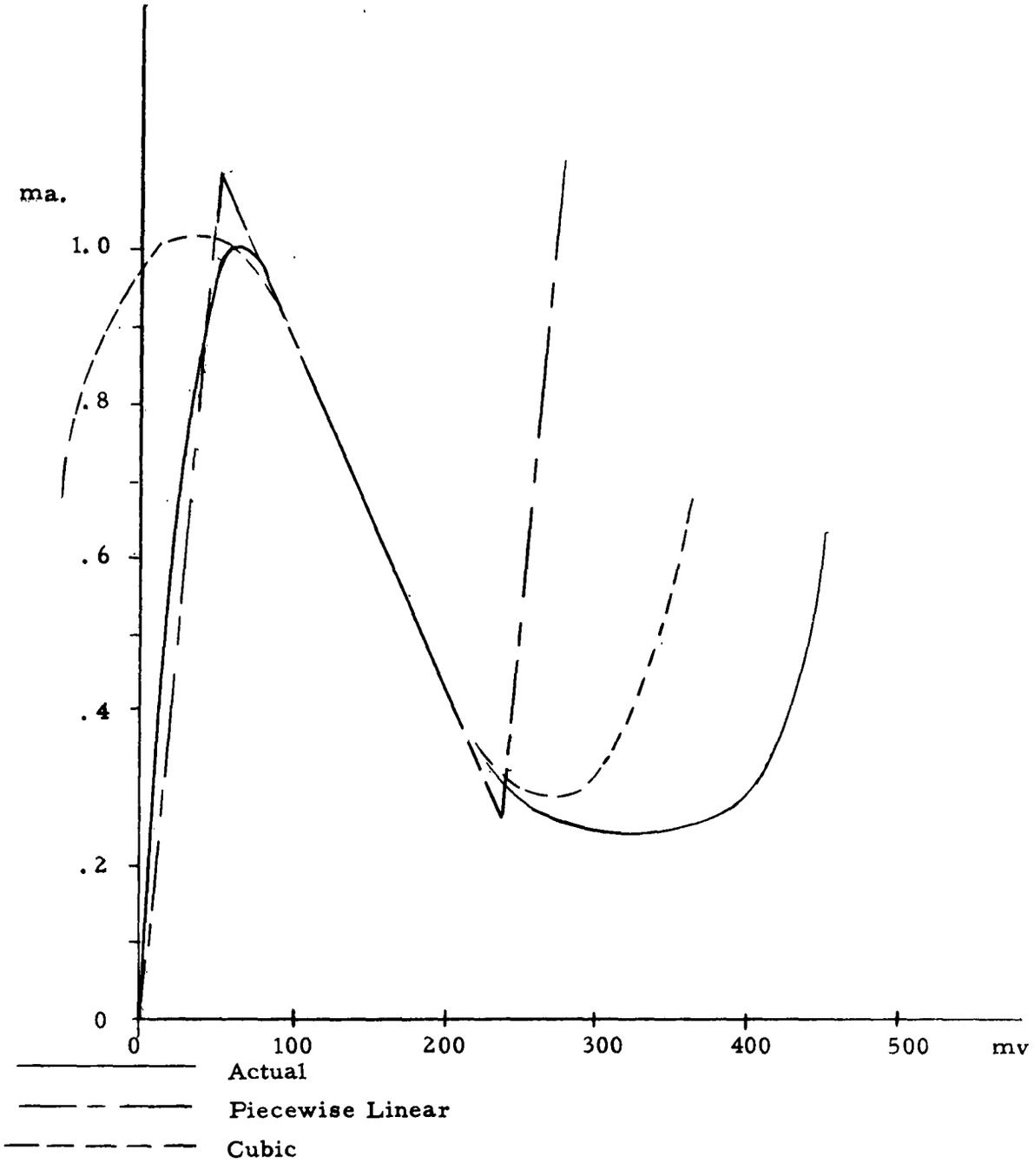

Figure 12b Static i-v Characteristics

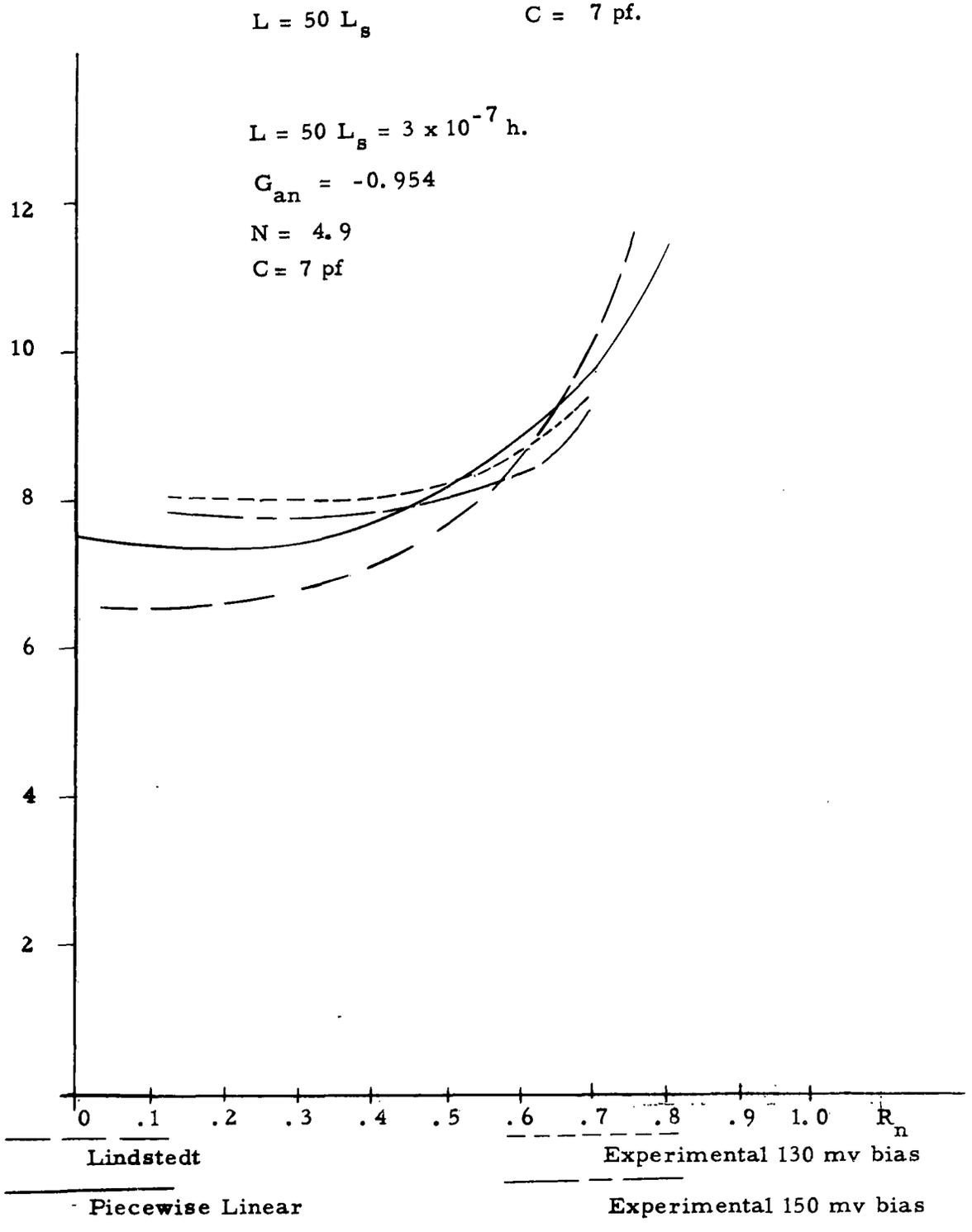

Figure 13 Experimental Results

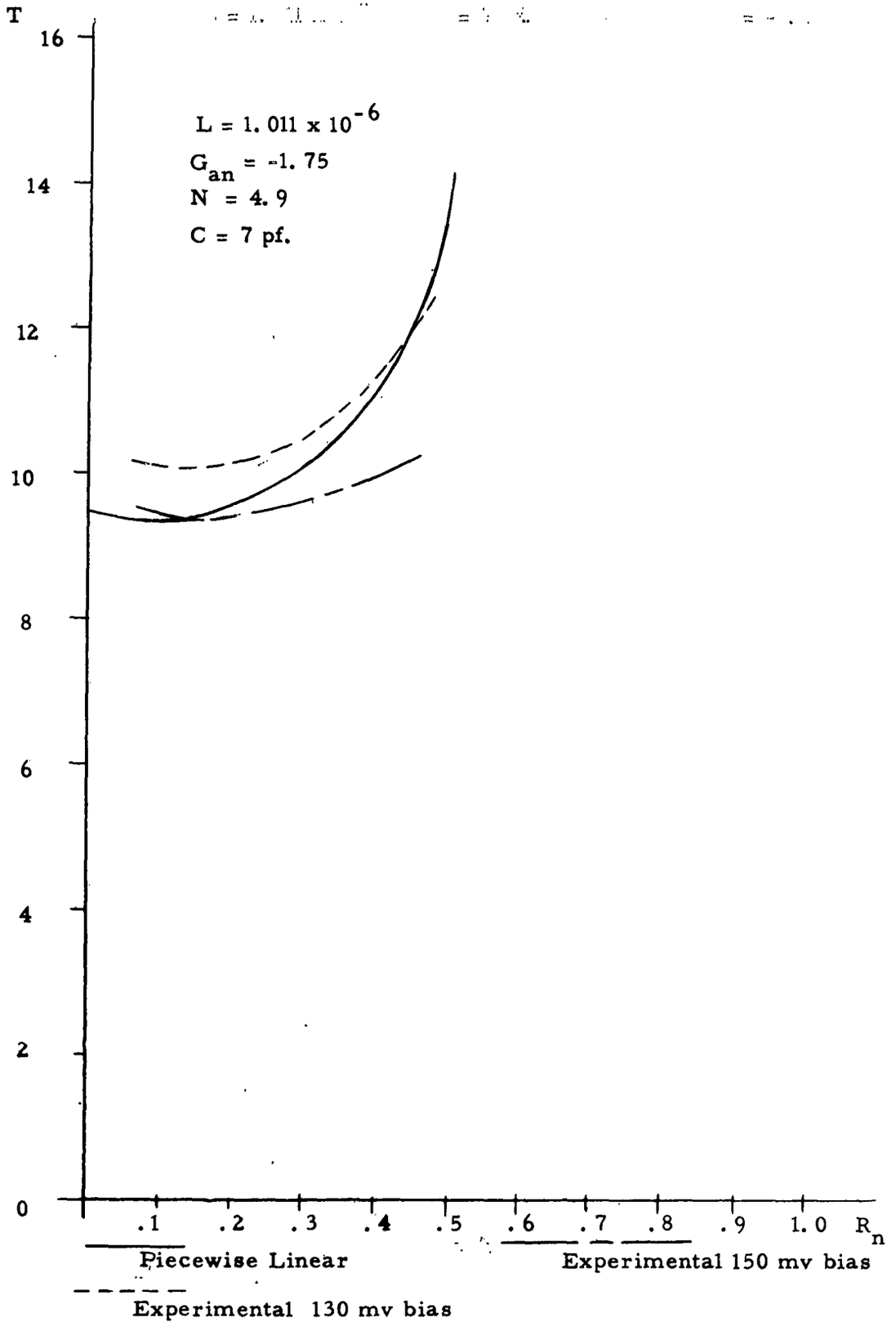

Figure 14 Experimental Results

REFERENCES

1. cf. - Sterzer, F., and Nelson, D. E. "Tunnel-Diode Microwave Oscillators," Proc. IRE, Vol. 49, No. 4 (April 1, 1961), pp. 744-753.

2. Shohat, J. "On Van der Pol's and Related Nonlinear Differential Equations," J. Appl. Phys., Vol. 15 (1944), p. 568.

3. Fisher, E. "The Period and Amplitude of the Van der Pol Limit Cycle," J. Appl. Phys., Vol. 25 (1954), p. 273.

4. Dorodnitsin, A. A. "Asymptotic Solution of the Van der Pol Equation," Inst. Mech. of the Acad. of Sci. of the U. S. S. R., Vol. 11 (1947).

5. Haag, J. "Examples concrets d'etude asymptotique d'oscillations de relaxation," Ann. Sci. Ecole Norm. Sup., Vol. 61 (1944).

6. Stoker, J. Nonlinear Vibrations, New York: Interscience Pub., 1950, p. 146.

7. In a recent paper, a perturbation analysis for the tunnel diode oscillators was made. However, certain significant terms were omitted which lead to the Van der Pol formulation and to erroneous conclusions.
   cf. - Schuller, M. and Gaertner, W. "Large-Signal Theory for Negative-Resistance Diodes in Particular Tunnel Diodes," Proc. IRE, Vol. 49, No. 8 (August 1961), pp. 1268-1278.

8. Minorsky, N. Introduction to Nonlinear Mechanics, chapter 11, "Approximations of Higher Orders." See also, chapter 10, "Theory of the First Approximation of Kryloff and Bogoliuboff," J. W. Edwards, 1947.

DISTRIBUTION LIST
AF 49(638)-1043

ORGANIZATION	NO. COPIES
Advanced Research Projects Agency Washington 25, D. C.	1
Aeronautical Research Laboratories Attn: Technical Library, Bldg. 450 Wright-Patterson Air Force Base Ohio	1
Applied Mechanics Reviews Southwest Research Institute 8500 Culebra Road San Antonio 6, Texas	1
ARO, Inc. Attn: AEDC Library Arnold Air Force Station Tullahoma, Tennessee	1
ASTIA Attn: TIPCR Arlington Hall Station Arlington 12, Virginia	10
Prof. N. Bloembergen Department of Physics Harvard University Cambridge 38, Massachusetts	1
Prof. Harvey Brooks Department of Physics Harvard University Cambridge 38, Massachusetts	1
Chairman, Canadian Joint Staff For DRB/DSIS 2450 Massachusetts Ave., N.W. Washington 25, D. C.	1
Chief, Physics Branch Division of Research U.S. Atomic Energy Commission Washington 25, D. C.	1
Commandant Air Force Institute of Technology (AU) Library, MCLI-LIB, Bldg. 125, Area B Wright-Patterson Air Force Base Ohio	1
Commander Air Force Cambridge Research Laboratories Attn: CRREL L.G. Hanscom Field Bedford, Massachusetts	1
Commander Air Force Flight Test Center Attn: FTOTL Edwards Air Force Base California	1
Commander Air Force Missile Development Center Attn: HDOI Holloman Air Force Base New Mexico	1
Commander Air Force Office of Scientific Research Attn: SRY Washington 25, D. C.	3
Commander Air Force Research Division Attn: RRRTL Washington 25, D. C.	2
Commander Air Force Special Weapons Center Attn: SWOI Kirtland Air Force Base New Mexico	1
Commander Air Research and Development Command Attn: RDR Andrews Air Force Base Washington 25, D. C.	2
Commander Air Research and Development Command Attn: RDRA Andrews Air Force Base Washington 25, D. C.	1
Commander Air Research and Development Command Attn: RDRB Andrews Air Force Base Washington 25, D. C.	1
Commander Air Research and Development Command Attn: RDRC Andrews Air Force Base Washington 25, D. C.	1
Commander Air Research and Development Command Attn: RDRS Andrews Air Force Base Washington 25, D. C.	1
Commander Army Rocket and Guided Missile Agency Attn: ORDXR-OTL Redstone Arsenal Alabama	1
Commander, Detachment 1 Hq. Air Force Research Division The Shell Building Brussels, Belgium	2
Commander Rome Air Development Center Attn: RAYLD Griffiss Air Force Base Rome, New York	1
Commander Wright Air Development Division Attn: WWAD Wright-Patterson Air Force Base Ohio	4
Commanding General U.S. Army Signal Corps Research and Development Laboratory Attn: SIGFM/EL-RPO Fort Monmouth, New Jersey	1
Director, Army Research Office Attn: Scientific Information Branch Department of the Army Washington 25, D. C.	1
Director, Department of Commerce Office of Technical Services Washington 25, D. C.	1
Director, Naval Research Laboratory Attn: Technical Information Officer Washington 25, D. C.	1
Director, Office of Ordnance Research Box CM, Duke Station Durham, North Carolina	1
Director of Research and Development Headquarters, USAF Attn: AFDRD Washington 25, D. C.	1
General Electric Company Electron Tube Division of the Research Laboratory The Knolls Schenectady, New York Attn: E. D. McArthur	1
Dr. Harold Glaser Office of Naval Research Washington 25, D. C.	1
Harvard University Gruft Laboratory Cambridge 38, Massachusetts Attn: Technical Reports Collection	1
Hughes Aircraft Company Florence at Teale St. Culver City, California Attn: Documents Group, Bldg. 6, Rm. X2015	1
Institute of Aeronautical Sciences Attn: Librarian 2 East 64 St. New York 16, New York	1
Prof. Zohrab Kaprielian University of Southern California School of Engineering Department of Electrical Engineering University Park Los Angeles 7, California	1
Prof. P. Kusch Department of Physics Columbia University New York 27, New York	1
Massachusetts Institute of Technology Research Laboratories of Electronics Room 20B-221, Document Office Cambridge 39, Massachusetts Attn: J. H. Hewitt	1
Hans Motz Oxford University Oxford, England	1
National Aeronautics and Space Administration Washington 25, D. C.	6
National Bureau of Standards Library Room 203, Northwest Building Washington 25, D. C.	1
Office of Naval Research Department of the Navy Attn: Code 420 Washington 25, D. C.	1
Ohio State University Department of Electrical Engineering Columbus, Ohio	1
Mr. E. Okress Sperry Gyroscope Company Electron Tube Division Mail Station IB40 Great Neck, New York	1
Physics Program National Science Foundation Washington 25, D. C.	1
P.O. Box AA Wright-Patterson Air Force Base Ohio	1
RCA Laboratories Princeton, New Jersey Attn: Dr. W. M. Webster, Director Electronics Research Laboratories	1
Dr. Irving Rowe Office of Naval Research 346 Broadway New York, New York	1
Sylvania Electric Company Mountain View, California Attn: D. H. Goodman	1
Technical Information Libraries Bell Telephone Laboratories, Inc. Whippany Laboratory Whippany, New Jersey Attn: Technical Reports Librarian	1
Prof. Charles Townes Department of Physics Columbia University New York 27, New York	1
University of Illinois Department of Electrical Engineering Urbana, Illinois Attn: H. Von Foerster	1
The University of Michigan Department of Electrical Engineering Electron Physics Laboratory Ann Arbor, Michigan Attn: Prof. J. E. Rowe	1
U.S. Atomic Energy Commission Technical Information Extension P.O. Box 62 Oak Ridge, Tennessee	1
Varian Associates 611 Hansen Way Palo Alto, California Attn: Technical Library	1
Westinghouse Electric Corp. Electronic Tube Division P.O. Box 284 Elmira, New York Attn: Mr. Sheldon S. King, Librarian	1
M. D. Adcock, Head Microwave Systems and Components American Systems, Inc. 3412 Century Boulevard Inglewood, California	1
Antenna Laboratory Electrical Engineering Research Laboratory University of Illinois Urbana, Illinois Attn: Dr. P. E. Mayes	1
Antenna Laboratory Ohio State University Research Foundation Columbus, Ohio Attn: Dr. C. T. Tai	1
Assistant Secretary of Defense Research and Development Board Department of Defense Washington 25, D. C.	1
Bell Telephone Laboratories, Inc. Central Serial Records Technical Information Library 463 West St. New York 14, New York	1
Boeing Aircraft Company Physical Research Unit Seattle 14, Washington Attn: Mr. R. W. Ilman	1
Dr. C. J. Bouwkamp Philips Research Laboratories N. V. Philips Gloeilampenfabrieken Eindhoven, Netherlands VIA ONR London	1
Brooklyn Polytechnic Institute Microwave Research Institute 55 Johnson St. Brooklyn 1, New York Attn: Dr. A. Oliner	1
California Institute of Technology Pasadena, California Attn: C. H. Papas	1
Cambridge University Radiophysics Division Cavendish Laboratory Cambridge, England VIA ONR London Attn: Mr. J. A. Ratcliffe	1
Chalmers Institute of Technology Goteborg, Sweden VIA ONR London Attn: Prof. S. Ekelof and Prof. H. Wallman	1
Chief, Bureau of Aeronautics Navy Department Washington 25, D. C. Attn: EL-51	1
Chief, Bureau of Ships Navy Department Washington 25, D. C. Attn: Code 838	2
Chief of Naval Research Navy Department Washington 25, D. C. Attn: Code 427	2
Chief of Naval Research Navy Department Washington 25, D. C. Attn: Code 460	1
Commander Air Force Office of Scientific Research Air Research and Development Command Washington 25, D. C.	1
Columbia Radiation Laboratories Columbia University 538 W. 120th St. New York 27, New York Attn: Librarian	1
Commander Naval Air Development Center Johnsville, Pennsylvania Attn: AEEL	1
Commander U.S. Naval Electronics Laboratory San Diego, California	1
Commanding General Rome Air Development Center Griffiss Air Force Base Rome, New York Attn: RCRW	1
Commanding General Signal Corps Engineering Laboratories Evans Signal Laboratory Area Building 27 Belmar, New Jersey Attn: Technical Documents Center	1
Commanding General Signal Corps Engineering Laboratories Fort Monmouth, New Jersey Attn: SIGEL-SMB-mf, MOB-Magnetic Materials	1
Commanding General Wright Air Development Center Wright-Patterson Air Force Base Ohio Attn: WCREO-2	1
Commanding Officer Squier Signal Laboratory Fort Monmouth, New Jersey Attn: V. J. Kubtin	1
Prof. N. DeClaris Cornell University Ithaca, New York	1
Department of Electrical Engineering Cornell University Ithaca, New York Attn: Dr. H. G. Booker	1
Department of Electrical Engineering Yale University New Haven, Connecticut	1
Director, Naval Research Laboratory Washington 25, D. C. Attn: Code 2000	1
Director, Naval Ordnance Laboratory White Oak, Maryland	1
Director, Naval Research Laboratory Washington 25, D. C. Attn: Code 5250	1
Douglas Aircraft Co., Inc. El Segundo Division El Segundo, California	1
Electrical Engineering Department Illinois Institute of Technology Technology Center Chicago 16, Illinois	1
Electrical Engineering Department University of Texas Box F, University Station Austin, Texas	1
Electronics Research Laboratory Stanford University Stanford, California Attn: Applied Electronics Laboratory Documents Library	1
Federal Telecommunications Laboratories, Inc. 500 Washington Ave. Nutley, New Jersey Attn: A. K. Wing	1

ORGANIZATION	NO. COPIES
Georgia Institute of Technology Atlanta, Georgia Attn: Mrs. J. Fenley Crosland, Librarian	1
Carl A. Hedberg, Head Electronics Division Denver Research Institute University of Denver Denver, Colorado	1
Hughes Aircraft Company Antenna Research Department Bldg. 12, Room 2617 Culver City, California	1
Hughes Aircraft Company Research and Development Library Culver City, California Attn: John T. Milek	1
Library Boulder Laboratories National Bureau of Standards Boulder, Colorado Attn: Victoria S. Barker	2
Mathematics Research Group New York University 25 Waverly Place New York, New York Attn: Dr. M. Kline	1
Mr. Frank J. Mullin Department of Electrical Engineering California Institute of Technology Pasadena, California	1
Naval Air Missile Test Center Point Mugu, California	1
Office of the Chief Signal Officer Pentagon Washington 25, D. C. Attn: SIGET	1
Office of Technical Services Department of Commerce Washington 25, D. C.	1
Radiation Laboratory Johns Hopkins University 1315 St. Paul St. Baltimore 2, Maryland Attn: Librarian	1
The Rand Corporation 1700 Main St. Santa Monica, California Attn: Margaret Anderson, Librarian	1
Randall Morgan Laboratory of Physics University of Pennsylvania Philadelphia 4, Pennsylvania	1
Regents of the University of Michigan Ann Arbor, Michigan	1
Research Laboratory of Electronics Document Room Massachusetts Institute of Technology Cambridge 39, Massachusetts Attn: Mr. J. Hewitt	1
Prof. Vincent C. Rideout Department of Electrical Engineering University of Wisconsin Madison 6, Wisconsin	1
Royal Technical University Laboratory for Telephony and Telegraphy Ostervoldgade 10 Copenhagen, Denmark VIA ONR London Attn: Prof. H. L. Knudsen	1
Prof. Samuel Seely, Head Department of Electrical Engineering Case Institute of Technology University Circle Cleveland 6, Ohio	1
Signal Corps Engineering Laboratories Fort Monmouth, New Jersey Attn: Mr. O. C. Woodyard	1
Stanford Research Institute 974 Commercial Stanford, California Attn: Dr. John T. Bolljohn Division of Electrical Engineering	1
Technical Reports Collection 303A Pierce Hall Harvard University Cambridge 38, Massachusetts	1

ORGANIZATION	NO. COPIES
Technical University Department of Electrical Engineering Delft, Holland VIA ONR London Attn: Prof. J. P. Schouten	1
University of Florida Gainesville, Florida Attn: Applied Electronics Laboratory Document Library	1
U.S. Naval Post Graduate School Monterey, California Attn: Librarian	1
Watson Laboratories Library AMC, Red Bank, New Jersey Attn: ENAGSI	1
Willow Run Research Center University of Michigan Ypsilenti, Michigan Attn: Dr. K. Siegel	1
Advisory Group on Electron Tubes 346 Broadway New York 13, New York	2
Bell Telephone Laboratories Murray Hill, New Jersey Attn: Dr. W. Kluver	1
California Institute of Technology Electron Tube and Microwave Laboratory Pasadena, California Attn: Prof. R. Gould	1
Chief, Bureau of Ships Department of the Navy Washington 25, D. C. Attn: 691A4	1
Chief of Ordnance Washington 25, D. C. Attn: ORDTX-AR	1
Chief of Research and Development OCS, Department of the Army Washington 25, D. C.	1
Chief Signal Officer Department of the Army Washington 25, D. C. Attn: SIGRD	1
Chief, U.S. Army Security Agency Arlington Hall Station Arlington 12, Virginia	2
Commander Air Force Command and Control Development Division Air Research and Development Command United States Air Force Laurence G. Hanscom Field Bedford, Massachusetts Attn: CROTL	1
Commander Wright Air Development Division Attn: WCOSI-3 Wright-Patterson Air Force Base Ohio	2
Commanding Officer Diamond Ordnance Fuze Laboratories Washington 25, D. C. Attn: Library, Rm. 211, Bldg. 92	1
Commanding Officer Frankford Arsenal Philadelphia 37, Pennsylvania Attn: ORDBA-FEL	1
Commanding Officer and Director U.S. Navy Electronics Laboratory San Diego 52, California	1
Commanding Officer, 9560th TSU U.S. Army Signal Electronics Research Unit P.O. Box 205 Mountain View, California	1
Commanding Officer U.S. Army Signal Material Support Agency Attn: SIGMS-ADJ	1
Commanding Officer U.S. Army Signal Research and Development Laboratory Fort Monmouth, New Jersey Attn: Director of Research	1
Commanding Officer Office of Naval Research, Branch Office 1000 Geary St. San Francisco 9, California	1

ORGANIZATION	NO. COPIES
Commanding Officer U.S. Army Signal Research and Development Laboratory Fort Monmouth, New Jersey Attn: Technical Documents Center	1
Commanding Officer U.S. Army Signal Research and Development Laboratory Fort Monmouth, New Jersey Attn: SIGRA/SL-PRM (Records File Copy)	1
Commanding Officer U.S. Army Signal Research and Development Laboratory Fort Monmouth, New Jersey Attn: Logistics Division (For SIGRA/SL-PRM) (Project Engineer)	2
Commanding Officer U.S. Army Signal Research and Development Laboratory Fort Monmouth, New Jersey Attn: Technical Information Division (FOR RETRANSMITTAL TO ACCREDITED BRITISH AND CANADIAN GOVERNMENT REPRESENTATIVES AND TO DEPARTMENT OF COMMERCE)	5
Deputy President U.S. Army Security Agency Board Arlington Hall Station Arlington 12, Virginia	1
Director, U.S. Naval Research Laboratory Washington 25, D. C. Attn: Code 2027	1
The European Office U.S. Army R and D Liaison Group APO 757 New York, New York (FOR RETRANSMITTAL TO CONTRACTOR, DA 91-591-EUC-1312)	1
Hughes Aircraft Company Culver City, California Attn: Dr. Mendel, Microwave Tube Laboratory	1
Marine Corps Liaison Office U.S. Army Signal Research and Development Laboratory Fort Monmouth, New Jersey	1
Massachusetts Institute of Technology Research Laboratory of Electronics Cambridge, Massachusetts Attn: Prof. L. Smullin	1
OASD (R and E), Rm. 3E1065 The Pentagon Washington 25, D. C. Attn: Technical Library	1
Radio Corporation of America Laboratories Princeton, New Jersey Attn: Dr. L. S. Nergaard	1
Raytheon Manufacturing Company Microwave and Power Tube Operations Waltham 54, Massachusetts Attn: W. C. Brown	1
Research Division Library Raytheon Company 28 Seyon St. Waltham 54, Massachusetts	1
S.F.D. Laboratories, Inc. 800 Rahway Ave. Union, New Jersey	1
Stanford University Electronic Research Laboratory Palo Alto, California Attn: Prof. D. A. Watkins	1
Sylvania Electric Products Physics Laboratory Bayside, Long Island, New York Attn: L. R. Bloom	1
U.S. Navy Electronics Liaison Office U.S. Army Signal Research and Development Laboratories Fort Monmouth, New Jersey	1
Watkins-Johnson Company 333 Hillview Ave. Stanford Industrial Park Palo Alto, California	1
Westinghouse Electric Corporation Research Laboratory Beulah Road, Churchill Boro Pittsburgh 35, Pennsylvania	1